Chapter 5

Experimental Results

5.1 Bunsen Type Burner Measurements

5.1.1 Global chemiluminescence measurements

Global chemiluminescence measurements on the Bunsen type burner were limited on the lean side to an equivalence ratio of 0.75, because blow–off for the burner occurred near an equivalence ratio of 0.7, depending on flow–rate. Similar blow–off limits were observed in the experimental apparatus of Sun et al. (1994). On the rich side, the measurements were made to an equivalence ratio of 1.1. The interest in rich chemiluminescence data is purely academic because generally gas turbine combustors are operated near lean blow–off. It is expected that the rich chemiluminescence data will help provide a more solid foundation for the understanding of chemiluminescence formation. The range of flow–rates studied is from 55 cc/sec of air–flow to 70 cc/sec of air–flow. A wider range of flow–rates would have required a flow–rate dependent narrowing of the range of equivalence ratios studied. The flow–rate variation is based on air–flow but clearly, the fuel–flow and total flow are directly related and could also be used as independent variables in any plots of the results.

OH^* chemiluminescence

The results for the OH^* chemiluminescence yield variation with equivalence ratio for all flow–rates studied are shown in Figure 5.1. The maximum for the chemiluminescence is located near stoichiometric mixture conditions. The decrease in chemiluminescence on the rich side is somewhat less steep than on the lean side. The dependence of OH^* on equivalence ratio resembles that of laminar flame–speed on equivalence ratio.(Turns, 1998) The variation of OH^* chemiluminescence yield with air–flow is shown in Figure 5.2, for the two equivalence ratios of 0.8 and 1.0. The variation with air–flow appears to be at least close to linear. The slope of the line varies with equivalence ratio. The variation of the slope with equivalence ratio is related to the variation of chemiluminescence yield with equivalence ratio. The slope is steepest at an equivalence ratio of 1.0, which corresponds to the maximum chemiluminescence yield when the equivalence ratio is varied. In order to better understand OH^* chemi-

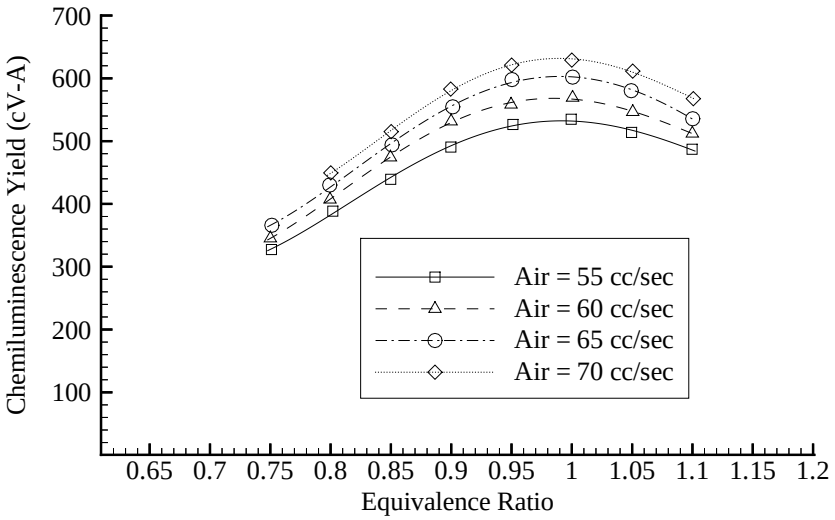

Figure 5.1: OH* chemiluminescence yield as a function of equivalence ratio

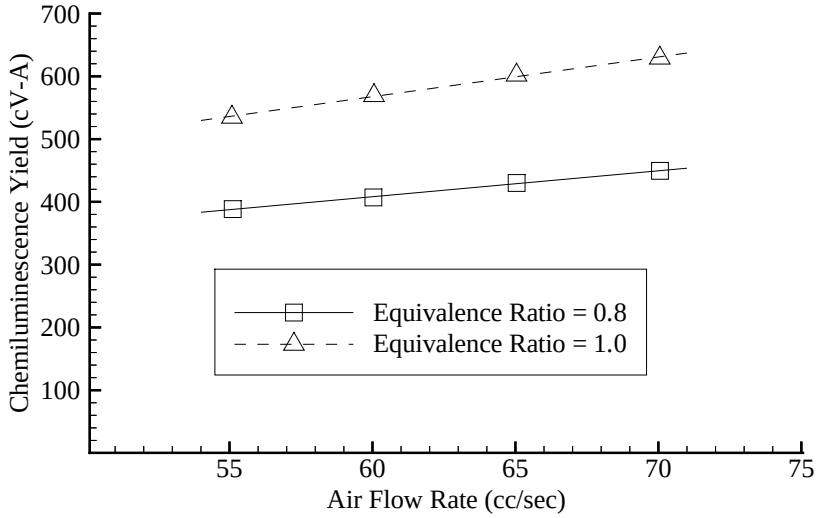

Figure 5.2: OH* chemiluminescence yield as a function of air–flow

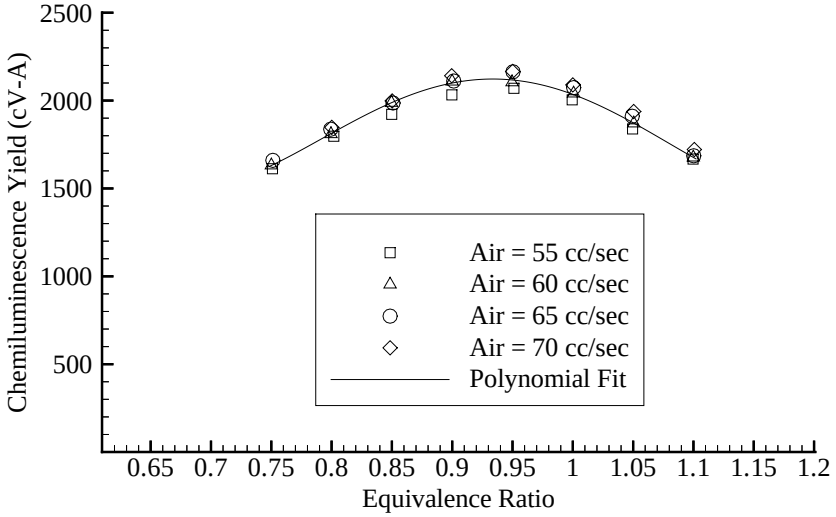

Figure 5.3: Normalized OH^* chemiluminescence yield as a function of equivalence ratio

luminescence formation an attempt was made to collapse the 2-D data (variation with equivalence ratio and air–flow) onto one curve describing the variation of a normalized chemiluminescence with equivalence ratio only. Figure 5.2 seems to indicate that the variation with flow–rate is linear and so, a division by air–flow or fuel–flow should allow the data to collapse onto the desired single curve. Although, the data shows less scatter, a deterministic variation with flow rate can still be detected. Full collapse is obtained when the OH^* is normalized not only by the fuel–flow but also by the square–root of the Reynolds number. The fuel flow–rate normalized chemiluminescence is multiplied by the Reynolds number. The result of the normalization is shown in Figure 5.3. The scatter seen along the curve does not contain a pattern, indicating that the scatter is purely due to random data–error. One conclusion from the normalization immediately evident is that OH^* chemiluminescence is not a linear function of fuel flow–rate. Other implications of the normalization used and its justification are discussed in detail in Section 10.1.1.

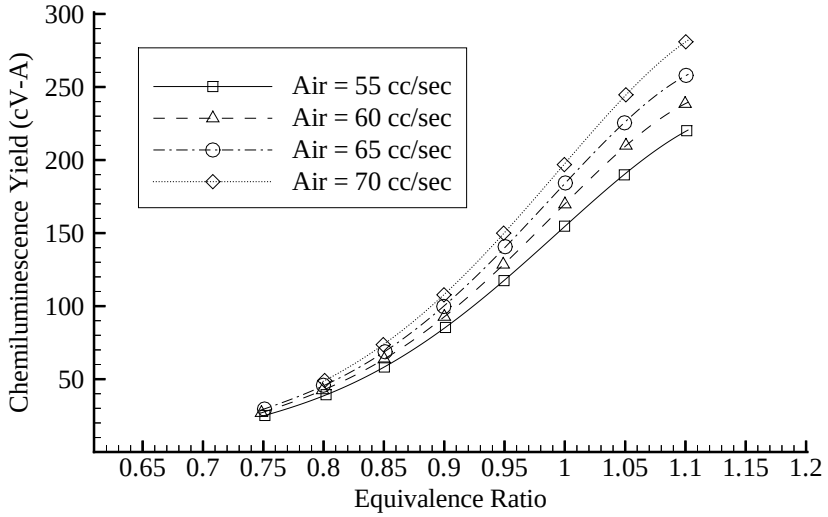

Figure 5.4: CH^* chemiluminescence yield as a function of equivalence ratio

CH^* chemiluminescence

The CH^* chemiluminescence variation with equivalence ratio for all flow–rates studied is shown in Figure 5.4. CH^* behaves very differently from OH^*. The peak for CH^* chemiluminescence lies on the rich side, beyond the range of the experimental conditions studied. As stoichiometric conditions are approached from the lean side, a near exponential dependence on equivalence ratio is found. The exponential dependence is not surprising considering the high activation energy required for the production of CH^* precursors. Based on the fact that the production path includes a two–carbon atom radical, the peak should be expected for fuel–rich mixtures. Although some introduction to the formation path of CH^* was given in Section 1.3.2, full discussion is reserved until Section 9.2. The variation of CH^* chemiluminescence with flow–rate for two equivalence ratios is shown in Figure 5.5. Here, as for OH^* chemiluminescence, the variation with air–flow appears to be linear with the slope of the line depending on equivalence ratio. The differences in the slope between the equivalence ratios shown can again be related to the variation of CH^* chemiluminescence with equivalence ratio. The higher the relative chemiluminescence yield, the steeper

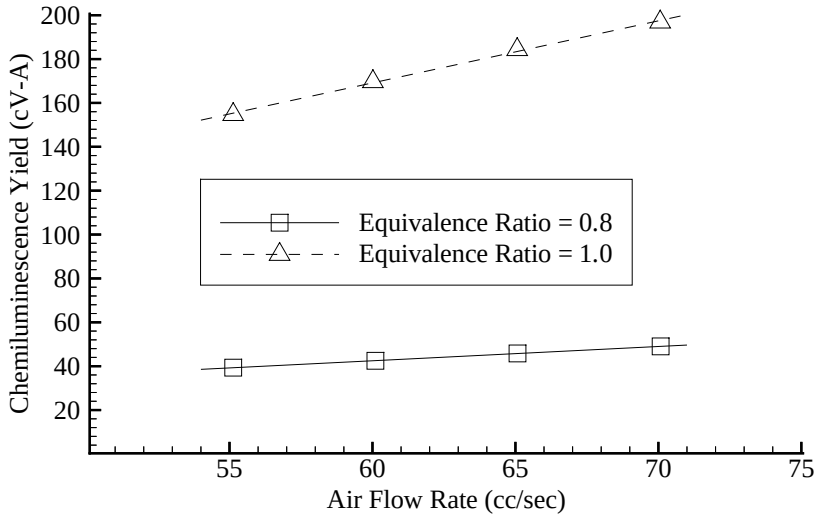

Figure 5.5: CH* chemiluminescence yield as a function of air flow–rate

the slope of the line in Figure 5.5. Paralleling the OH* chemiluminescence data presentation, an attempt is made to collapse the data for CH* chemiluminescence onto one curve describing the dependence of a normalized CH* chemiluminescence yield solely on equivalence ratio. The first clear dependence is on flow–rate and all CH* measurements were normalized by fuel–flow. The normalization results in the collapse of all flow–rates onto one curve as shown in Figure 5.6. The normalization for CH* chemiluminescence is different from the normalization used in the case of OH* chemiluminescence. The normalization used indicates that CH* chemiluminescence is indeed a linear function of fuel flow–rate. Comparison to OH* and further discussion of the matter is deferred to Section 10.1.1.

Chemiluminescence ratio

Based on the results shown above, the ratio of OH* chemiluminescence to CH* chemiluminescence can be expected to be a unique function of equivalence ratio. Using normalized values of chemiluminescence in the ratio would yield a better fit

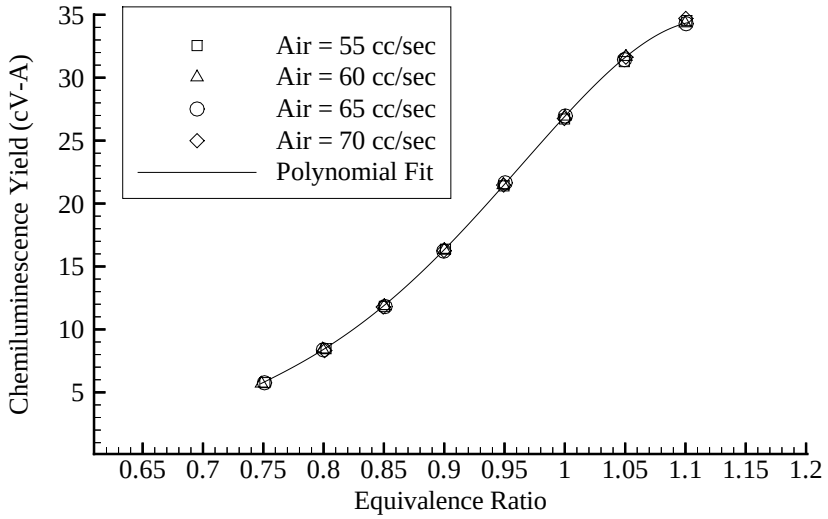

Figure 5.6: Normalized CH^* chemiluminescence yield as a function of equivalence ratio

but in an attempt to provide results that will apply to any burner, the unnormalized chemiluminescence yields will be used in the evaluation of the ratio. The resulting curve is plotted in Figure 5.7.

5.1.2 Local chemiluminescence measurements

Local chemiluminescence measurements were performed to get a qualitative insight into the burning of a Bunsen flame. The collected voltages are corrected with the same factors as the global chemiluminescence measurements, even though the optical system is not identical (see Section 4.3.2). The error introduced by using the same correction factor is of no consequence in the qualitative deductions made based on the local chemiluminescence data.

All of the collected data shown in Figures 5.8 through 5.11 is non-smooth and asymmetric with respect to the flame center. The asymmetry is due to an actual burning asymmetry of the flame. The asymmetry is caused by the inability to provide a completely circumferentially even co–flow. Deductions based on global chemiluminescence measurements are not affected by the slight asymmetry. The apparent

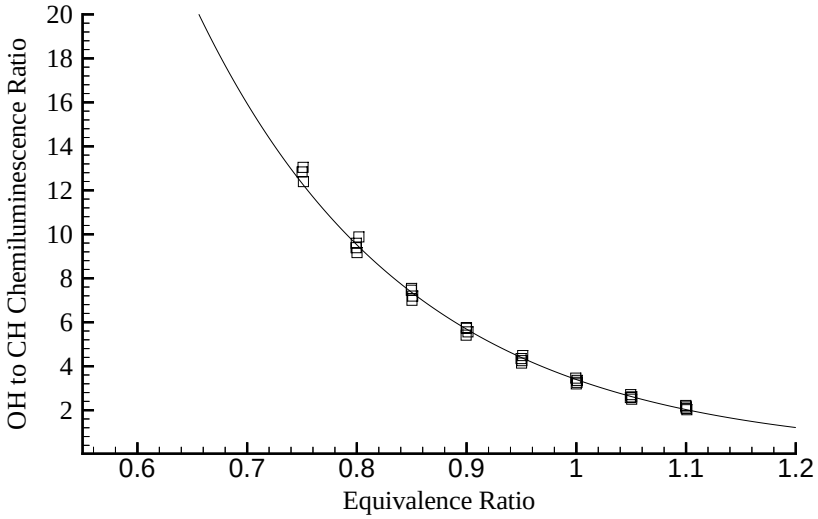

Figure 5.7: Ratio of OH* to CH* chemiluminescence yields as a function of equivalence ratio

discontinuities in the data have to do with the fact that only a very small amount of light is collected and noise contaminates the signal collected.

OH* chemiluminescence

The radial variation of OH* chemiluminescence for three equivalence ratios at an air flow–rate of 60 cc/sec is shown in Figure 5.8. The variation of chemiluminescence over the radius of the flame is significant. The chemiluminescence increases from near zero to a maximum and then shows a local minimum in the center of the flame. The chemiluminescence variation is affected by the flame shape as well as the interaction between the main combustion flow and the co–flow of air. The basic shape remains constant for all equivalence ratios. The scaling is similar to that observed for global chemiluminescence with the maximum chemiluminescence being emitted for the stoichiometric flame, and less for the lean and rich flames. The radial variation of OH* chemiluminescence for two different air flow–rates at an equivalence ratio of 1.0 is shown in Figure 5.9. The shape observed in Figure 5.8 remains the same for changes in air flow–rate. Note that the difference between the two curves is very small consid-

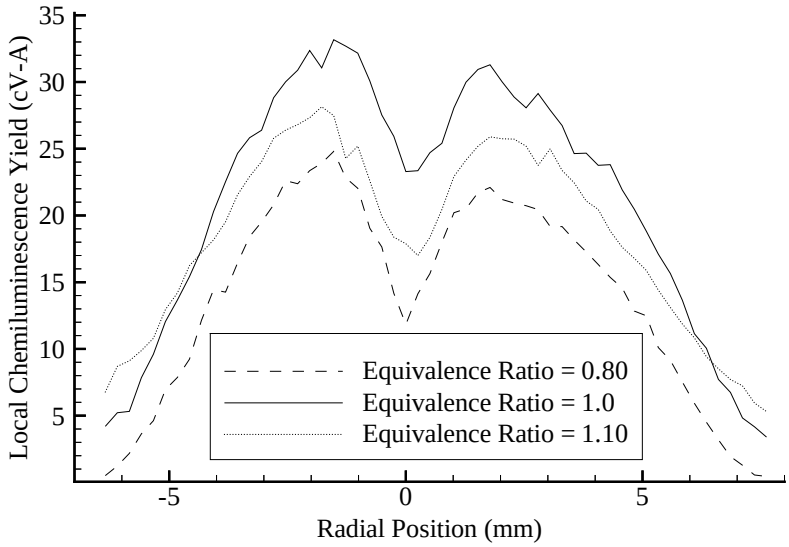

Figure 5.8: Radial variation of OH* chemiluminescence with equivalence ratio at an air flow–rate of 60 cc/sec

ering the 15% increase in air flow–rate between the two curves. However, the increase in chemiluminescence with flow–rate is clearer when the intensity is integrated. Recall as well that the same 15% increase in air–flow was only seen to increase the global chemiluminescence measurement by 9% in Figure 5.2.

CH* chemiluminescence

The radial variation of CH* chemiluminescence for three equivalence ratios at an air flow–rate of 60 cc/sec is shown in Figure 5.10. The variation of chemiluminescence over the radius of the flame is again significant. The shape of the CH* chemiluminescence variation is very similar to that of OH* chemiluminescence. The shape is invariant to changes of equivalence ratio. The shape scales to other equivalence ratios approximately like the global CH* chemiluminescence with the maximum emission (for studied equivalence ratios) at an equivalence ratio of 1.10. The radial variation of CH* chemiluminescence for two different air flow–rates at an equivalence ratio of 0.80 is shown in Figure 5.11. The shape observed in Figure 5.10 remains the same for changes in air flow–rate with increases in air flow–rate resulting in higher chemilu-

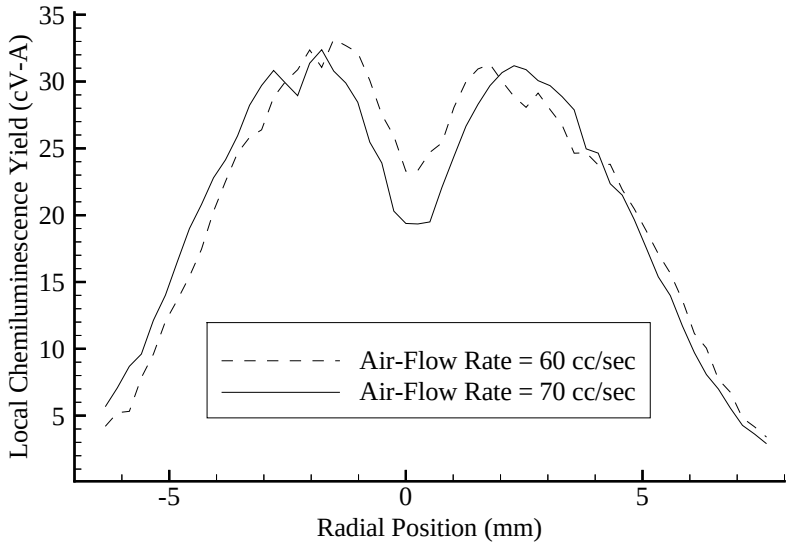

Figure 5.9: Radial Variation of OH^* chemiluminescence with air flow–rate at an equivalence ratio of 1.0

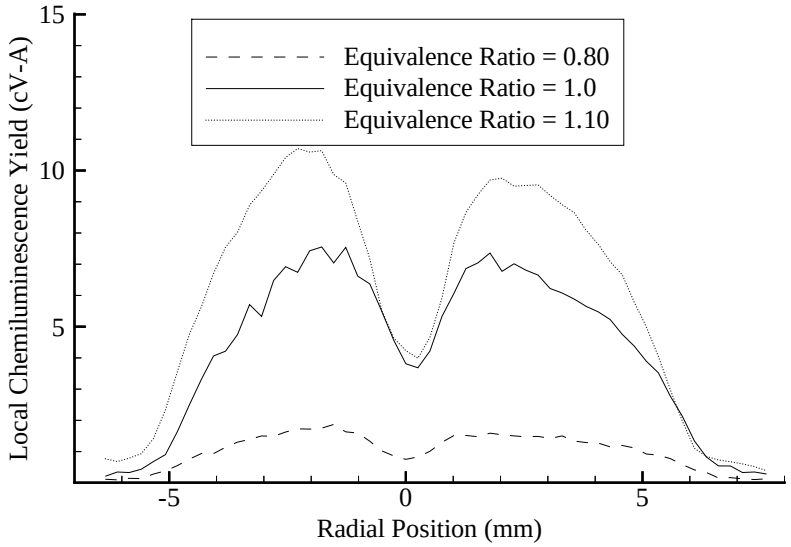

Figure 5.10: Radial Variation of CH^* chemiluminescence with equivalence ratio at an air flow–rate of 60 cc/sec

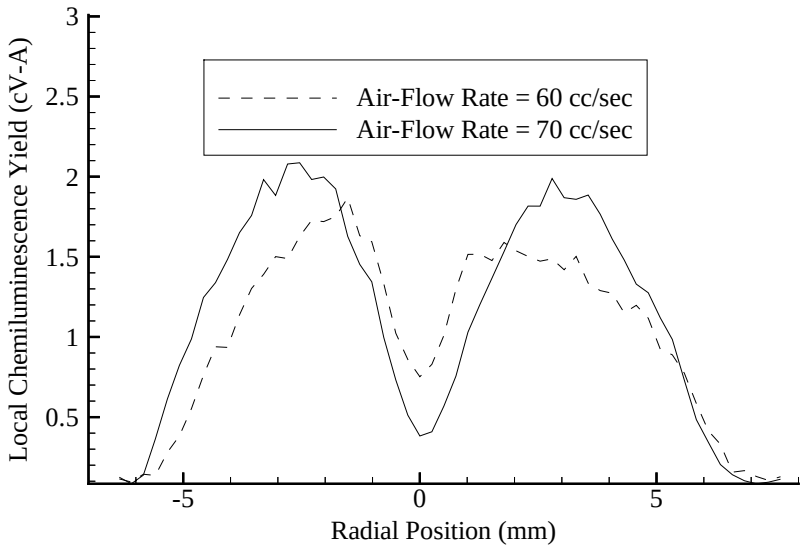

Figure 5.11: Radial Variation of CH^* chemiluminescence with air flow–rate for an equivalence ratio of 0.80

minescence emission. The difference in CH^* chemiluminescence observed for the two flow–rates is much greater than the difference in OH^* chemiluminescence observed for the same change in flow–rate in Figure 5.9. The difference in behaviour between OH^* and CH^* chemiluminescence can be explained by pointing out that while the 15% increase in flow–rate only causes a 9% increase in integrated OH^* chemiluminescence the same increase in flow–rate causes a 17% increase in integrated CH^* chemiluminescence.

Radial variation of chemiluminescence ratio

For global chemiluminescence, it is found that the ratio of OH^* chemiluminescence to CH^* chemiluminescence is a good indicator of equivalence ratio at all flow rates. To obtain a qualitative insight into how the air co–flow affects the Bunsen flame, the same ratio is plotted over the radius of the flame. The variation of the ratio along the radius is shown in Figure 5.12 for several equivalence ratios at an air flow–rate of 60 cc/sec. The figure shows shapes that are approximately inverted from those seen for example in Figure 5.11. According to Figure 5.7, higher values of the

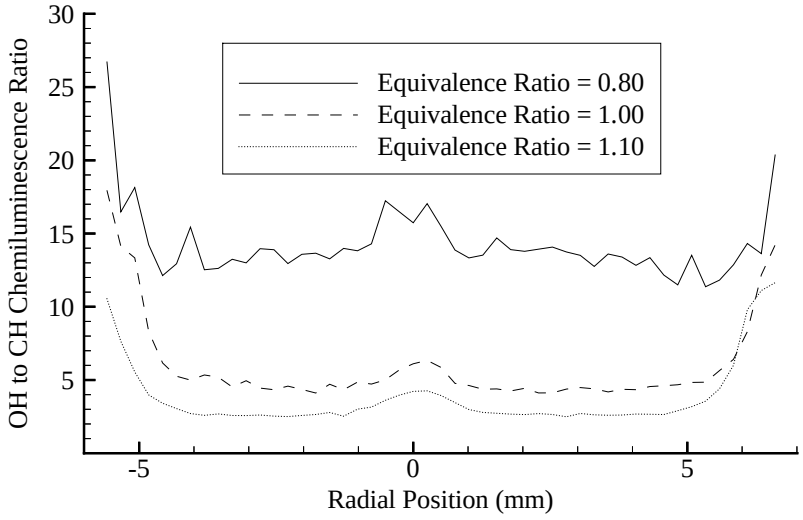

Figure 5.12: Radial Variation of the ratio of OH^* to CH^* chemiluminescence for several equivalence ratios

ratio indicate leaner equivalence ratios. The outer edges of the flame consistently show very high values of the ratio, indicative of air from the co–flow mixing with the premixed air and fuel prior to burning. Details of the mixing and burning processes will be discussed in further detail in Section 7.3.1 with respect to the semi-empirical Bunsen burner model. The variation of the ratio in the center of the flame will be discussed further in Section 7.5.3.

5.2 Honeycomb Burner Measurements

The motivation for taking these measurements is to provide a large database of chemiluminescence results for a full chemistry 1-D model, discussed in Chapter 8. The data will help to elucidate the formation path for OH^* chemiluminescence. The honeycomb burner was operated at equivalence ratios between 0.6 and 1.10 with air flow–rates varying from 130 cc/sec to 270 cc/sec. The data for 270 cc/sec was limited to equivalence ratios below 0.925 because a burner instability sets in above this equivalence ratio. Unfortunately Measurements for the honeycomb burner are

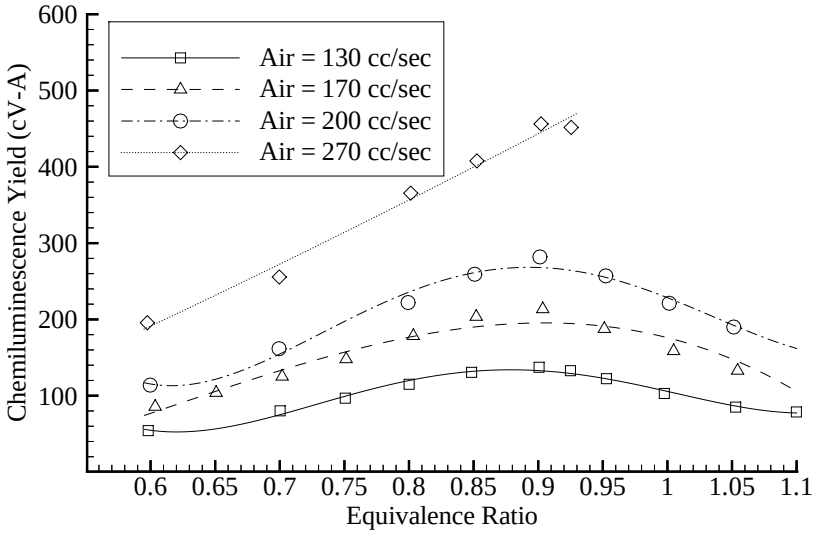

Figure 5.13: Variation of OH* chemiluminescence with equivalence ratio

limited to global chemiluminescence measurements.

5.2.1 OH* chemiluminescence

The variation of OH* chemiluminescence yield with equivalence ratio for several air flow–rates is shown in Figure 5.13. Peak OH* chemiluminescence for the honeycomb burner is observed near an equivalence ratio of 0.90. The rate of decline of OH* emission for leaner mixtures is about equal to the rate of decline of emission for richer mixtures. As the air flow–rate is increased chemiluminescent emission increases and the shape of the curve stays approximately the same.

It was not possible to collapse the OH* chemiluminescence data in a fashion similar to the Bunsen type burner. Nevertheless, it is important to show that the dependence of OH* chemiluminescence, on a per unit mass of fuel basis, is still a function of the fuel flow–rate. The resulting curve of fuel flow–rate specific OH* chemiluminescence versus fuel flow–rate is shown in Figure 5.14. Again it is important to note that OH* chemiluminescence is found not to be a linear function of fuel

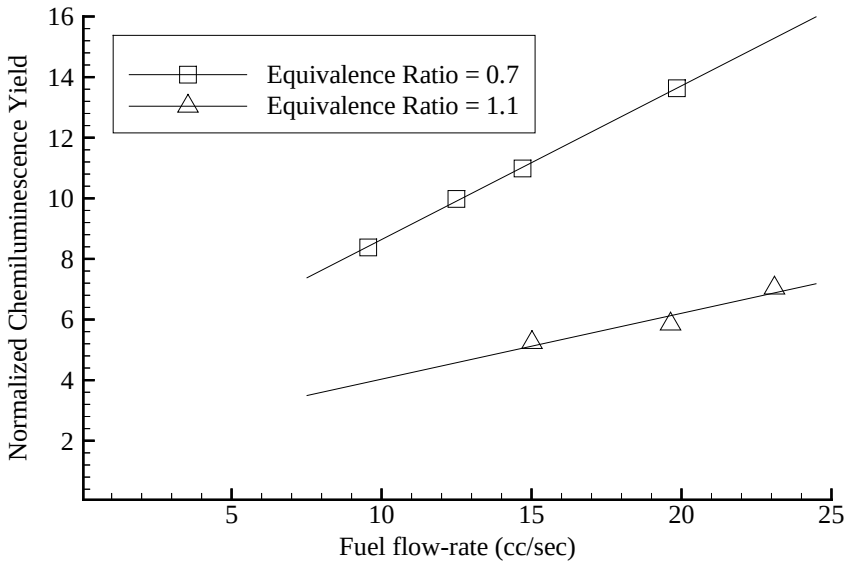

Figure 5.14: Variation of normalized OH* chemiluminescence with fuel flow–rate

flow–rate. The implications and physical explanation will be discussed in detail in Section 10.1.2.

5.2.2 CH* chemiluminescence

The variation of CH* chemiluminescence yield with equivalence ratio for several air flow–rates is shown in Figure 5.15. Peak CH* chemiluminescence for the honeycomb burner is observed near an equivalence ratio of 1.0. The decline of CH* emission for leaner mixtures is much steeper than the decline of emission for richer mixtures. The emission of CH* chemiluminescence almost appears to be leveling off for equivalence ratios above 1.0. As the air flow–rate is increased chemiluminescent emission increases and the shape of the curve stays approximately the same. Similar to the OH* chemiluminescence data for the honeycomb burner, the CH* chemiluminescence data for the honeycomb burner can also not be collapsed. However, again in parallel to the OH* chemiluminescence data, the fuel flow–rate specific CH* chemiluminescence is found to be still a function of the fuel flow–rate. The resulting curve is shown in Figure 5.16. The variation of CH* chemiluminescence with fuel flow–rate is

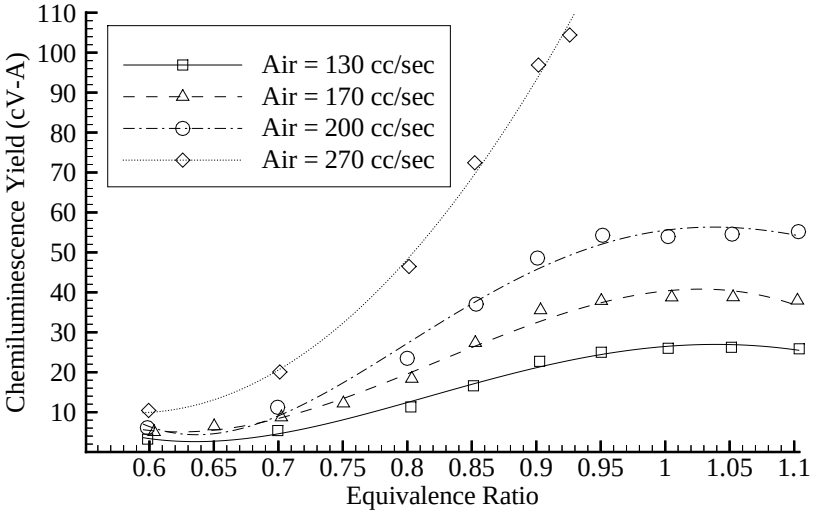

Figure 5.15: Variation of CH* chemiluminescence with equivalence ratio

thus not linear, in contrast to the Bunsen burner. Further implications and physical interpretation of the results will be discussed in detail in Section 10.1.2.

5.2.3 Chemiluminescence ratio for the honeycomb burner

Figure 5.17 shows the ratio of OH* chemiluminescence to CH* chemiluminescence for all global chemiluminescence data collected, i.e. for both the honeycomb and Bunsen type burners. The curve shows that even though the data collected stems from different burners, operated at very different conditions, the ratio of the two types of chemiluminescence studied appears to be a unique function of equivalence ratio. The result will be further discussed in Section 10.5.

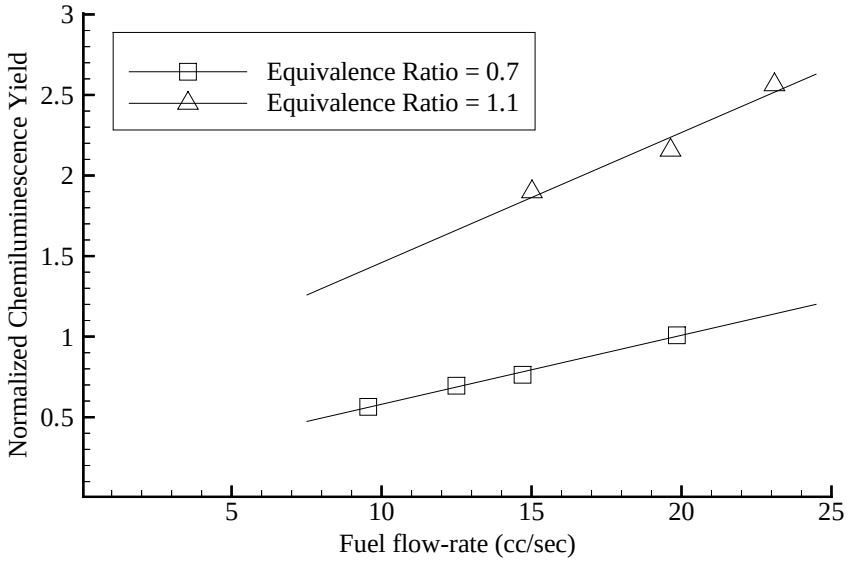

Figure 5.16: Variation of normalized CH^* chemiluminescence with fuel flow–rate

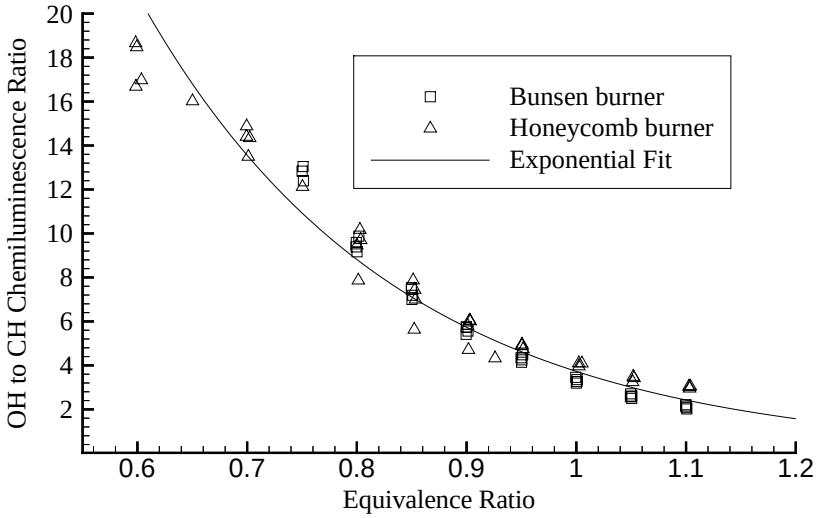

Figure 5.17: Variation of OH^* to CH^* chemiluminescence ratio with equivalence ratio

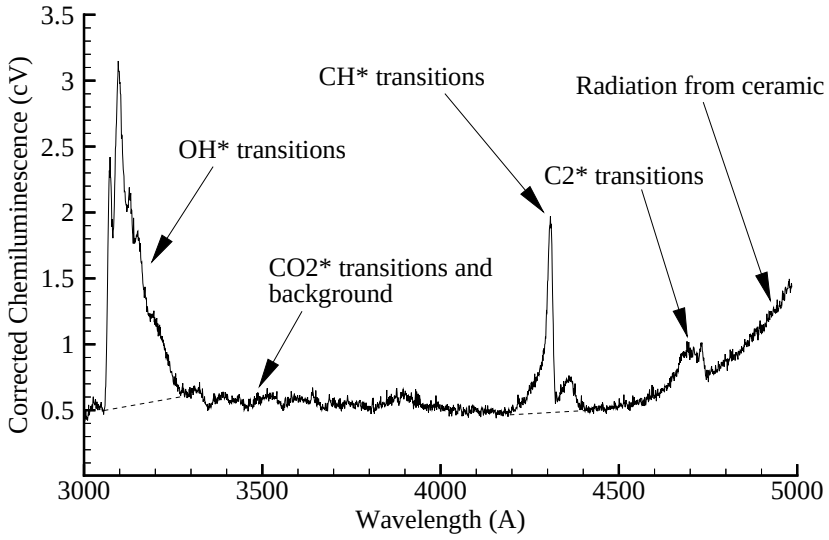

Figure 5.18: Spectral wavelength scan of the honeycomb burner

5.2.4 Light emission spectra for the honeycomb burner

The honeycomb burner spectral scans exhibit an interesting feature that has important implications for other radiative environments such as gas turbines. A spectral scan of the honeycomb at an air flow–rate of 200 cc/sec with an equivalence ratio of 1.00 is shown in Figure 5.18. Just beyond the CH^* peak at 4310 A, a continuous increase in the voltage is observed. The energy that generates the increase seen originates from the honeycomb. Had the burner been running any hotter, the radiation may have begun to contaminate the collected CH^* chemiluminescence signal. Radiative contributions from other materials in the combustor as well as other gases in the combustor are not always negligible. Caution must be exercised in all combustion environments to assure that the radiative energy collected has the desired origin, namely the flame reaction zone. Collection of chemiluminescence data using wider band–pass filters, like the ones sometimes used to measure CO_2^* (Najm et al., 1998) are especially susceptible to radiation contamination.